GA–A25658

PRECISION X-RAY OPTICAL DEPTH MEASUREMENTS IN ICF SHELLS

by

S.A. EDDINGER, R.B. STEPHENS, H. HUANG, T.J. DRAKE, A. NIKROO,
G. FLINT, and C.R. BYSTEDT

JANUARY 2007

GENERAL ATOMICS

DISCLAIMER

GA–A25658

PRECISION X-RAY OPTICAL DEPTH MEASUREMENTS IN ICF SHELLS

by
S.A. EDDINGER, R.B. STEPHENS, H. HUANG, T.J. DRAKE, A. NIKROO, G. FLINT, and C.R. BYSTEDT

This is a preprint of a paper presented at the 17th Target Fabrication Specialist Meeting, San Diego, California on October 1-5, 2006 and to be published in *Fusion Science and Technology.*

Work supported by
the U.S. Department of Energy
under DE-AC52-06NA27279

GENERAL ATOMICS PROJECT 30272
JANUARY 2007

PRECISION X-RAY OPTICAL DEPTH MEASUREMENTS IN ICF SHELLS

S.A. Eddinger, R.B. Stephens, H. Huang, T.J. Drake, A. Nikroo, G. Flint, and C.R. Bystedt

General Atomics, P.O. Box 85608, San Diego, California 92186-5608
eddinger@fusion.gat.com

We built a precision radiography system that measures shells for all current ablator materials to an accuracy of 1:10^4 in optical depth fluctuation and a spatial resolution of 120 μm. The data obtained by the precision radiography system for undoped shells was compared with the data taken using the well-known surface measurement technique Spheremapper. Since both techniques yielded the same power spectrum for the same shell, the results of the precision radiography system were verified. When this technique is compared to the Be:Cu NIF shell, there is no significant internal layer fluctuation. To account for the growing measurement demand, a new x-ray system to accommodate measurements in 1 working day was designed.

I. INTRODUCTION

Rayleigh-Taylor instability places stringent limitations on fluctuations of x-ray opacity thickness in National Ignition Facility (NIF) targets.[1] NIF shells were validated using the precision radiography system according to customer specification: optical depth fluctuations were measured to an accuracy of 1:10^4 and a spatial resolution was determined to 120 μm. The opacity of Inertial Confinement Fusion (ICF) shells forces this measurement to be made at much higher photon energies (~3 keV) than is relevant in an implosion (0.3–1 keV), but measurement can be directly related to the desired value.

The instrument utilizes an x-ray source, scintillator/ photomultiplier detector, and a data collection scheme that eliminates all but photon noise, as described in Sec. II. Its measurement accuracy is demonstrated in Sec. III, and measurements of a variety of sample targets are shown in Sec. IV. These results can be interpreted in terms of the sample structure; as described in Sec. V, the fluctuations are typically dominated by the outside surface roughness. The possibility of fine scale internal structure, hinted at in Be shell data, leads to a desire for improved spatial resolution. As described in Sec. VI, the improved design allows for increased special resolution at a cost of substantially increased measurement time.

II. SYSTEM DESIGN

Figure 1 shows a CAD diagram of the final system built to measure the shell described in Fig. 2, which has the x-ray absorption spectrum shown in Fig. 3. A low voltage x-ray source is necessary to maximize x-ray flux around 3 keV, where the transmission fraction is about 10% and where measurements are most sensitive. An aperture collimates this x-ray beam, preventing secondary collisions from being counted as background noise. These x-rays penetrate through the front and back surface of the shell, entering into a fast scintillator. The scintillator converts the x-ray energy photons into visible light. The emitted light is transmitted through back-to-back microscope objectives used as a 5× relay lens and focused on an 8×2 array of hexagonally closed packed 120 μm diameter fiber optic cables, which are each attached to independent photomultiplier tubes (PMT). This system covers more than 1 mm of the shell, more than halfway toward each pole. To give high precision transmission profiles along 16 paths covering more than half the shell, data was taken every 0.1° as the shell is rotated at 1 RPM on a shaft-encoded airbearing. Measuring the shell a second time, after a 90° rotation, allows for 97.5% shell coverage for the combined data sets.

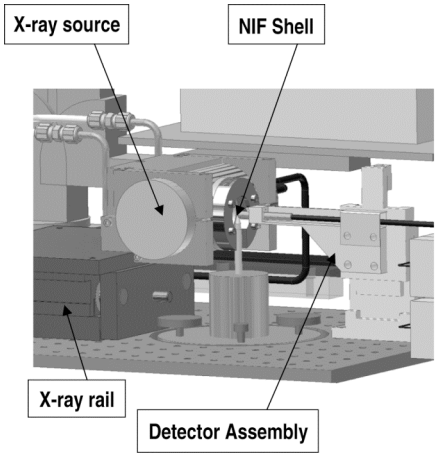

Figure 1. Precision radiography system design.

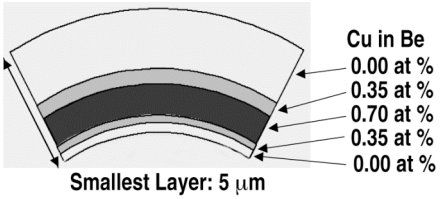

Figure 2. Current Be:Cu NIF design specification is 160 μm.

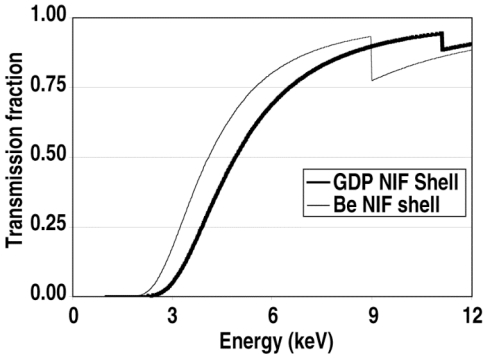

Figure 3. Be:Cu and GDP:Ge NIF ICF design shows 10% transmission fraction occurs near 3000 eV.

In order to get to higher measurement accuracy, all the systematic error mechanisms are eliminated. The three main mechanisms are electronic counting noise, x-ray spot drift, and shaft wobble.

To minimize electronic counting noise we use PMTs. The PMTs used have background counts of ~10 counts/s and can resolve 10^7 counts/s, which has a max accuracy of $1{:}10^6$ well below our specification of $1{:}10^4$.[2]

By interlacing data every minute, all of the effects of spot drift on the data are eliminated. If the system is rotated very slowly (~1/1000 RPM), the source intensity and location will change significantly from the first point to the last point. (Computed tomography reconstructions have issues with this.) As a result, the data from the first point to the last point will not accurately reflect the true profile of the shell. It is only through many quick, repeated measurements that the effects of this long-term source drift can be eliminated.

Another common problem is shaft wobble, which is the result of poor initial alignment on the rotation axis. This causes a mode 1 perturbation (measuring thicker and thinner regions of the shell) in shell measurement data, creating large artificial mode 1 optical depth variations. To minimize this perturbation, an integrated capacitive detector system[3] for aligning the vacuum post on the true rotation axis was implemented. It works by measuring distances to a smooth metal ball located on a vacuum shaft. The system minimizes the wobble to approximately 1 μm. This is an order of magnitude better than what can be achieved through optical alignment alone.

III. MEASUREMENT VERIFICATION

The measurement accuracy was validated using point-by-point ratioing of successive transmission measurements of a single shell. If all the systematic error mechanisms are eliminated, then the difference between two successive data sets is only system noise (Fig. 4). The quality of a measurement can be quantified by comparing the standard deviation of the empirical data with the theoretical photon noise.[4]

$$\text{True photon noise} = \sqrt{1/C_{\text{avg}}} \quad , \tag{1}$$

$$\text{Verification photon noise} = \sqrt{4/C_{\text{avg}}} \quad , \tag{2}$$

where C_{avg} is the average number of total measurement counts over all angles. Since two independent data sets are being compared, errors must be added in quadrature. As such, there is a factor of 2 in the square root. Since each data set is half the size of the total number, a second factor of 2 is introduced. Table I shows the noise is as expected from error analysis. This shows that the system does not have any significant systematic error. The error measured is $<1{:}10^4$, as required by the specification.

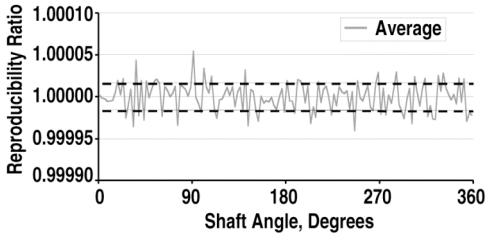

Figure 4. There is no systematic noise in this measurement when averaging all 16 PMT. The dashed lines correspond to the 1-σ standard deviation. As can be seen, all data is well within the required $1{:}10^4$ measurement error.

Table I. Experimental and Theoretical St. Deviation Show Very Good Agreement

	PMT 1 ($\times 10^{-05}$)	PMT 8 ($\times 10^{-05}$)	PMT 9 ($\times 10^{-05}$)	PMT 16 ($\times 10^{-05}$)
Empirical	6.45	5.75	5.41	5.19
Theoretical	5.89	5.06	5.42	4.86

IV. X-RAY TRANSMISSION MEASUREMENTS

Several of the possible ablator materials were studied: Ge doped GDP, Diamond, and Cu doped Be. As a simple test of the system, experiments were performed on different ablator materials to examine the count

uniformity as a function of angle. Each curve is normalized to its average value for ease of comparison. Figures 5–7 shows that significant features are easily identifiable when looking at the normalized transmission.

The GDP trace (Fig. 5) shows a large dip from a dome (~0.5 μm high) on the surface of the shell. Since the x-rays penetrate the entire shell, this dome is seen in two places, 180° apart. It also shows some mode 2, which corresponds to a slight ellipticity in the outer surface due to the coating process. This can be seen by the sinusoidal nature of the profile, with a dip at ~110° and a peak at ~200°.

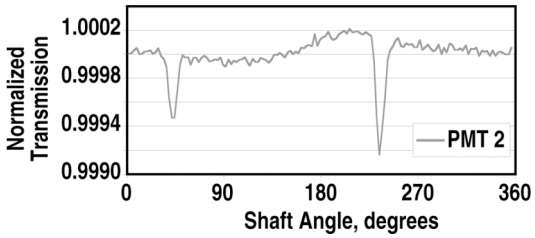

Figure 5. GDP shell measurement shows dome and mode 2 information.

The same analysis was conducted on the diamond shell (Fig. 6). This diamond shell was one of the first produced and polished. Diamond shells are much more absorbing of x-rays than GDP and Be. A 1% change in the normalized transmission corresponds to a 1% change in the thickness. The diamond shell has a 2-wall thickness of 200 μm, making the defect a 2 μm high dome, much larger than the GDP dome.

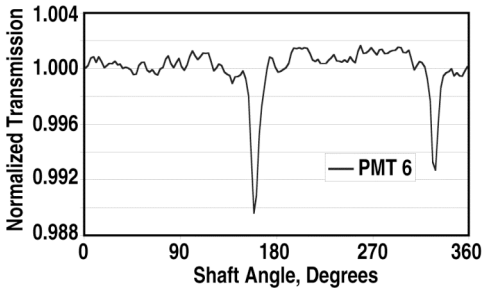

Figure 6. Diamond shell measurement shows large dome.

Three adjacent traces are shown for the undoped Be shell (Fig. 7); one can see that large features spread across adjacent independent data channels. The undoped shell shows many peaks and valleys that correspond to real transmission fluctuations. This is not surprising since the mandrel was of poorer quality then that used to make the GDP shell in Fig. 5.

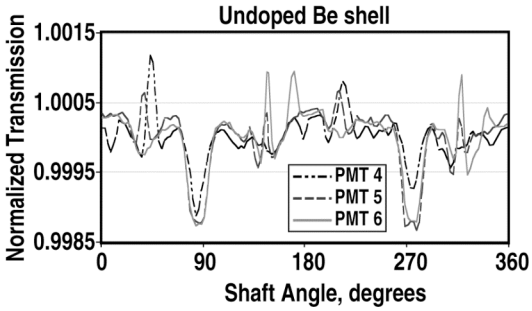

Figure 7. Be shell data shows that huge defects reproduce in adjacent PMTs.

V. APPLICATIONS

Precision radiography measures optical depth fluctuations of the shell. For undoped shells, the optical depth fluctuation can only be due to wall thickness uniformity. For a shell with a smooth inner surface, the wall thickness uniformity is a measure of the outer surface uniformity. Fortunately, the uniformity of a shell can be measured very accurately independently using Spheremapper. Therefore, precision radiography data can be benchmarked against the true surface uniformity data for an undoped shell.[5] The two methods are compared for undoped Be, GDP, and diamond shells [Fig. 8(a-c)]. There is some disagreement, as precision radiography shows additional structure above modes 20 for the undoped Be shell. However, the comparisons indicate that the precision radiography matches the data very well.

Doped shells can also be measured. The optical depth fluctuations can be due to dopant interfacial uniformity as well as thickness uniformity. Since Cu is more absorbing than Be in Be doped Cu shells, the effect of interface non-uniformity affects the bulk power spectra more then a non-uniformity in the outer surface. Figure 9 shows a doped Be shell coated to the specifications in Fig. 2. There is no significant difference between these two measurements except above mode 20 similar to the undoped Be case. This result is very encouraging; there is very little interfacial non-uniformity for this shell.

VI. IMPROVEMENTS NEEDED

It takes approximately 5 days to get high quality data regarding optical depth fluctuation and special resolution due to low x-ray tube brightness. Because these measurements are so important for shell characterization, the system was improved to decrease the measurement time so that shells can be routinely characterized in a day. The x-ray tube was redesigned to give 30× more flux, reducing the required counting time to 4 hours. Also, the system sensitivity was improved by choosing a Ag x-ray

source with the characteristic line at 3 keV optimized for Be:Cu and GDP:Ge shells.

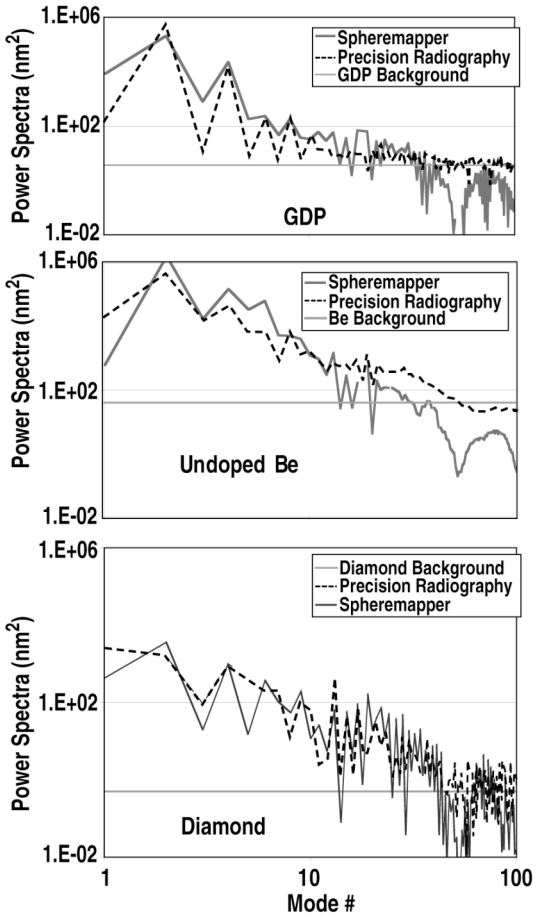

Figure 8. (a-c) Surface uniformity and precision radiography power spectra data show good agreement for all undoped shells. At higher modes, precision radiography hits its noise floor.

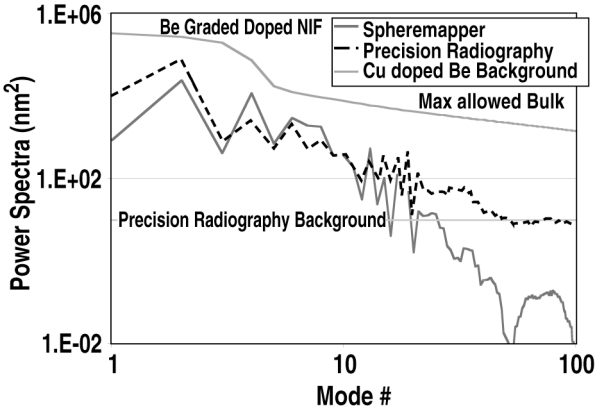

Figure 9. Be:Cu shell shows similar structure to undoped shell. The total profile is under the max allowed bulk specification for this sample.

To investigate the power spectra modal difference in Be (> mode 20), high modes must be accurately resolved. Due to the 120 μm resolution, the system is unable to measure information past mode 30. Figure 10 shows the effects of measuring increased times. The resolution of the system can be improved by purchasing smaller fiber optic cables, which enables higher mode measurements. However, because counts scale with the surface area, if the resolution is increased from 120 μm to 60 μm, the counting time must be increased by a factor of 4.

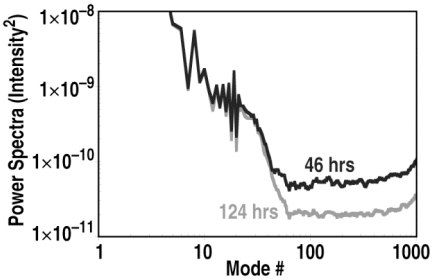

Figure 10. Despite increasing the time by a factor of 3, we obtain no additional modal information; we only reduce the photon noise floor.

VII. CONCLUSION

Precision radiography can measure a shell to 1:10^4 accuracy and a spatial resolution of 120 μm on all possible ablator materials. By comparing this measurement with the surface measurement Spheremapper, it was verified that the major non-uniformity for all undoped shells is due to surface fluctuations. By applying this technique to the Be:Cu NIF shell, no significant internal layer fluctuation was found. There is some structure at modes >20 and the system resolution will be increased to investigate this. To account for the growing measurement demand, a new Ag x-ray system was designed to accommodate measurements in one working day.

ACKNOWLEDGMENT

This work was supported by the U.S. Department of Energy under DE-AC52-06NA27279.

REFERENCES

1. M. D. ROSEN, "The Physics Issues That Determine Inertial Confinement Fusion Target Gain and Driver Requirements: A Tutorial," *Phys. Plasmas* **6**, 1690 (1999).

2. HAMAMATSU, H7155-20 PMT: http://www.hamamatsu.com.

3. CAPACITEC DETECTOR (HPC-40): http://www.capacitec.com/cfyl.htm.

4. PHOTON NOISE: http://en.wikipedia.org/wiki/Photon_noise

5. R. B. STEPHENS, D. OLSON, H. HUANG, J. B. GIBSON, "Complete Surface Mapping of ICF Shells," *Fusion Sci. Technol*. **45**, 210 (2004).